

## RESEARCH ARTICLE



# Disruption of focal adhesions by *Clostridioides difficile* TcdB variants

Deida Loáiciga-Rodríguez<sup>1</sup>, Iveth Jiménez-Badilla<sup>1</sup>, Carlos Quesada-Gómez<sup>1\*</sup>\*Correspondence: [quesada@ucr.acr](mailto:quesada@ucr.acr)<sup>1</sup>Facultad de Microbiología and Centro de Investigación en Enfermedades Tropicales, Universidad de Costa Rica, San José, Costa Rica.Submission December 13, 2025  
Accepted December 18, 2025  
Available online on April 30, 2026

©2026 The Authors. Published by Stem Cell and Cancer Research, Semarang, Indonesia. This is an open-access article under the terms of the Creative Commons Attribution-NonCommercial-ShareAlike License (CC BY-NC-SA 4.0), which permits unrestricted use, distribution, and reproduction in any medium, provided the original author and source are credited.

## ABSTRACT

**Background:** *Clostridioides difficile* infection (CDI) is a leading cause of antibiotic-associated nosocomial diarrhea, with disease severity predominantly influenced by the activity of toxin B (TcdB). Although TcdB-mediated inactivation of Rho family GTPases is well established, the downstream consequences for cell–matrix adhesion architecture remain poorly defined. **Objective:** This study examined how TcdB variants with distinct substrate specificities (VPI 10463, NAP1/RT027, and NAP1v/RT019) disrupt focal adhesion organization and cytoskeletal integrity. **Results:** Purified TcdB variants were standardized by functional equipotency and applied to HeLa cells. While most structural adhesion proteins, including talin and zyxin, demonstrated quantitative stability, plectin exhibited a selective and progressive loss following exposure to RhoA-inactivating toxins. Concurrently, paxillin phosphorylation was significantly diminished, and co-immunoprecipitation analyses disclosed a substantial dissociation of paxillin from pivotal adhesion components, with no indication of global proteolytic degradation. Morphological outcomes correlated with toxin substrate specificity: RhoA-inactivating variants resulted in cell rounding, while NAP1v promoted an arborizing phenotype. **Conclusion:** Collectively, these findings suggest that TcdB variants predominantly induce a biochemical disassembly of focal adhesion complexes rather than widespread protein degradation. This adhesion uncoupling mechanism may represent a molecular framework linking toxin specificity to epithelial barrier disruption and could potentially be associated with differences in clinical severity among CDI strains.

**Keywords:** *Clostridioides difficile*, focal adhesions, bacterial toxins.

## INTRODUCTION

*Clostridioides difficile* infection (CDI) has been identified as the primary cause of antibiotic-associated nosocomial diarrhea on a global scale. This opportunistic anaerobic bacterium colonizes the colon following dysbiosis of the intestinal microbiota, which is typically induced by broad-spectrum antibiotic therapy. The pathogenesis of the disease is primarily mediated by toxins A (TcdA) and B (TcdB). TcdB is regarded as the principal determinant of toxicity and clinical severity. It has been demonstrated that both toxins act as glycosyltransferases, which results in the inactivation of Rho family GTPases (RhoA, Rac1, and Cdc42). These GTPases are proteins that serve as central regulators of the actin cytoskeleton and cellular architecture<sup>1</sup>.

In recent decades, the emergence of the hypervirulent NAP1/RT027 strain has substantially altered the epidemiology of CDI. This strain has been associated with more severe outbreaks, increased toxin production, and higher mortality rates<sup>2</sup>. A critical feature of these variants is their substrate specificity: whereas conventional TcdB glycosylates RhoA, Rac1, and Cdc42, the TcdB variant associated with the NAP1/RT019 genotype lacks the ability to glycosylate RhoA.

This molecular difference translates into distinct cytopathic phenotypes, whereby toxins that inactivate RhoA induce pronounced cell rounding, whereas those that preserve RhoA activity generate an arborizing phenotype characterized by filiform actin-rich protrusions<sup>3</sup>. These effects demonstrate that toxin substrate specificity determines not only cellular morphology but also the functional impact on epithelial integrity.

Intestinal epithelial homeostasis is tightly dependent on the integrity of cell–matrix adhesions, which function as platforms for signaling and force transmission between the cell and its microenvironment. Focal adhesions (FAs) link the actin cytoskeleton to the extracellular matrix through multiprotein complexes organized around integrins, while adaptor proteins such as paxillin coordinate the dynamic assembly of the adhesome<sup>4</sup>. Likewise, structural proteins such as talin, zyxin, and plectin play key roles in the physical coupling of integrins to actin and intermediate filaments, thereby contributing to mechanical stability, and epithelial barrier function<sup>5,6</sup>.

The relevance of investigating how *C. difficile* toxins affect cellular adhesions lies in the fact that disruption of these proteins is directly linked to key pathological phenomena *in vivo*, including increased intestinal permeability, inflammation, and the formation of mucosal lesions<sup>7</sup>. Determining whether this disruption results from proteolytic degradation or from functional disassembly is critical for the design of therapeutic interventions and may provide molecular explanations for the differences in disease severity or recurrence observed among distinct clinical genotypes<sup>8</sup>.

The present study investigates the manner in which distinct TcdB variants (VPI 10463, NAP1/RT027, and NAP1v/RT019) disrupt cellular adhesions and cytoskeletal organization. A comparative analysis of key structural and adaptor proteins is employed to determine the origin of toxin-induced alterations, specifically whether they result from proteolytic degradation or functional uncoupling of adhesion complexes. This strategy establishes a correlation between toxin substrate specificity and the molecular and morphological changes underlying epithelial integrity loss in *C. difficile* infection.

## MATERIALS AND METHODS

### *Toxin purification*

TcdB toxins were purified from culture supernatants of well-characterized *C. difficile* strains using a sequential procedure that included dialysis for buffer exchange, ion-exchange chromatography, and gel filtration, in order to obtain highly enriched preparations that were comparable across variants. The strains used corresponded to VPI 10463 (conventional reference strain, clade 1), NAP1/RT027 (hypervirulent epidemic strain, clade 2), and NAP1v/RT019 (a clade 2 variant with altered substrate specificity)<sup>3,9</sup>.

The concentration of purified toxins was determined by referencing a reference toxin B (TcdB–VPI 10463), which served as a standard. The absolute concentration was previously established at 200 ng/μL through the use of Bradford Protein Assay (BioRad), with its reliability confirmed by comparison with bovine serum albumin standards. Quantification of TcdBs were performed by densitometric comparison on 7% SDS-PAGE gels stained with PageBlue (Thermo), ensuring detection within the linear range. Band intensities were interpolated against a standard curve generated using the reference toxin and analyzed with the ChemiDoc imaging system (BioRad)<sup>3</sup>.

Given that TcdB variants exhibit intrinsic differences in enzymatic activity and substrate specificity, particularly the inability of TcdB-NAP1v to glycosylate RhoA, the biological potency of the toxins was standardized according to a functional equipotency concept, in order to ensure temporal comparability of the observed molecular effects regardless of the applied protein mass<sup>3</sup>. To

this end, the 50% cytopathic concentration (CPE<sub>50</sub>) was determined in HeLa cells and defined as the minimal dose capable of inducing a cytopathic effect in 50% of the cell monolayer at a fixed time point, based on morphological criteria such as cell rounding, arborization, and detachment from the culture surface<sup>10</sup>. After performing serial dilutions in 96-well plates and monitoring the kinetics of the cytopathic effect over 6 hours, a dose of 50 ng per well was determined to achieve the CPE<sub>50</sub> precisely at 4 hours of exposure, thereby enabling detailed analysis of early molecular events preceding complete cellular collapse<sup>11</sup>.

### *Cell culture and toxin exposure*

HeLa cell cultures were maintained in DMEM/F12 medium supplemented with 10% fetal bovine serum (Sigma) until reaching approximately 90% confluence in 6-well plates. For intoxication assays, cells were incubated at 37 °C in a humidified atmosphere containing 5% CO<sub>2</sub> and exposed to 50 ng of the corresponding TcdB variant (VPI, NAP1, or NAP1v)<sup>3</sup>. The intoxication status was monitored by light microscopy using the following criteria: loss of fusiform morphology, appearance of cytoplasmic projections, cell rounding, and ultimately detachment from the culture surface. A particular focus was placed on the distinction between the arborizing effect, defined by the presence of dendritic-like protrusions, as observed with VPI and NAP1, and the perfect cell rounding induced by the NAP1v<sup>12</sup>. The toxin concentration of 50 ng/well was selected based on functional equipotency as previously characterized. This dose was shown to reach the CPE<sub>50</sub> at 4 h of exposure in HeLa cells, providing a consistent biological effect to analyze the early molecular disassembly of focal adhesions prior to complete cell detachment.

### *Preparation of cell lysates*

HeLa cells were washed with sterile PBS and lysed using 2% SDS lysis buffer supplemented with a complete EDTA-free protease inhibitor cocktail (Roche) and a phosphoSTOP phosphatase inhibitor cocktail (Roche). As with the experimental HeLa samples, both the negative control (HeLa cells treated with buffer only at 0 h) and the positive control (HeLa cells intoxicated with functional toxin) were lysed under the same conditions<sup>13</sup>. Lysate integrity was verified by total protein quantification using the DC Protein Assay kit (Bio-Rad) and by 10% SDS-PAGE analysis with staining performed for each HeLa cell lysate .

### *Detection of focal adhesion (FA) proteins*

For Western blot analyses, samples containing 50 µg of protein from HeLa cell lysates were prepared. The required volume of each lysate was calculated based on prior protein quantification, and the mixtures were adjusted with reducing loading buffer. HeLa cell samples were then boiled and centrifuged at 14,000 rpm. Proteins were resolved by 10% SDS-PAGE and transferred onto PVDF membranes<sup>3,15</sup>.

Then, FA proteins were detected by Western blot using polyclonal primary antibodies against FAK, paxillin, zyxin, plectin, ZO-1, and talin, as well as antibodies specific for the phosphorylated forms pTyr118-paxillin, pTyr527-Src, and pSer142-zyxin (Thermo Fisher Scientific). A polyclonal antibody against Src was also used (Cell Signaling). Subsequently, an HRP-conjugated anti-rabbit IgG secondary antibody (Thermo Fisher Scientific) was applied, and signal detection was performed by chemiluminescence using the Lumi-Light Western Blotting Substrate kit (Roche). Chemiluminescent signals were documented with ChemiDoc System (BioRad).

## Co-Immunoprecipitation (Co-IP) assays

Antibody coupling was performed by incubating a mouse monoclonal anti-paxillin antibody with Dynabeads Protein G (DPG) (Thermo), according to the manufacturer's instructions. Coupling was confirmed by detection of the paxillin band by Western blot in immunoprecipitates from control samples. Lysates incubated with DPG alone were used as negative control. Subsequently, HeLa cells (control and NAP1-intoxicated for 3 h) were lysed using cold RIPA buffer supplemented with protease and phosphatase inhibitors (Roche).

Lysates were centrifuged at 14,000 rpm for 15 min at 4 °C. For pull-down assays, clarified lysates were incubated with anti-paxillin-coupled DPG for 3 h at 4 °C. Beads were then washed with 50 mM Tris-HCl (pH 7.4), 150 mM NaCl, and 0.15% Triton X-100. The precipitated proteins were eluted by boiling in Laemmli sample buffer (Sigma) and subsequently resolved by SDS-PAGE for protein detection by Western blotting<sup>17,18</sup>.

## Image analysis

WB images analysis was performed using ImageJ. For each target protein band intensity was normalized to the intensity of the corresponding  $\alpha$ -actin loading control band. Densitometric values were reported in Table S1 and S2. Statistical comparisons were performed using one-way ANOVA followed by Tukey's multiple comparison test;  $p < 0.05$  was considered statistically significant.

## RESULTS

### Biological activity and CPE

After monitoring the CPE in HeLa cells every 30 minutes over a 6-hour period, a dose of 50 ng per well was determined to be optimal for reaching the CPE precisely at 4 hours of exposure, thereby enabling accurate characterization of intoxication progression.

### Detection and integrity status of FA protein components following toxin exposure

The structural components analyzed, including talin, zyxin, ZO-1, and  $\alpha$ -actinin, maintained constant expression levels throughout the 0–4 h time course under all conditions evaluated. This finding suggests that these components remain within the cell despite the cell rounding observed.

Nevertheless, among all focal adhesion proteins analyzed, plectin was the only one that exhibited a progressive decrease in band intensity as exposure time increased, becoming barely detectable from 2 h onward following treatment with TcdB-VPI and TcdB-NAP1. In addition, a late reduction (3–4 h) in total paxillin band intensity was specifically observed upon exposure to the reference VPI toxin (Fig. 1).

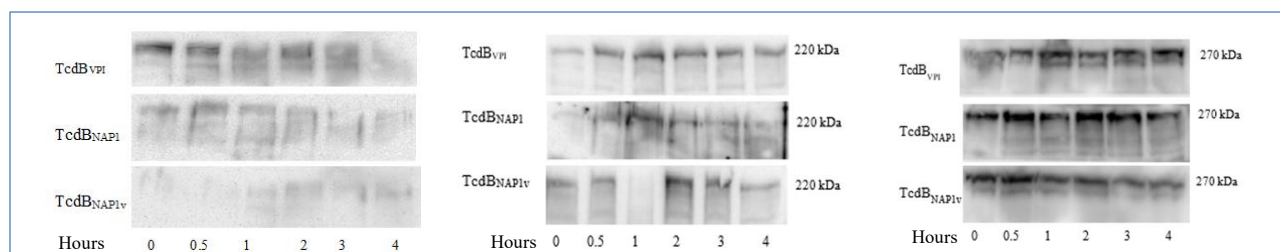
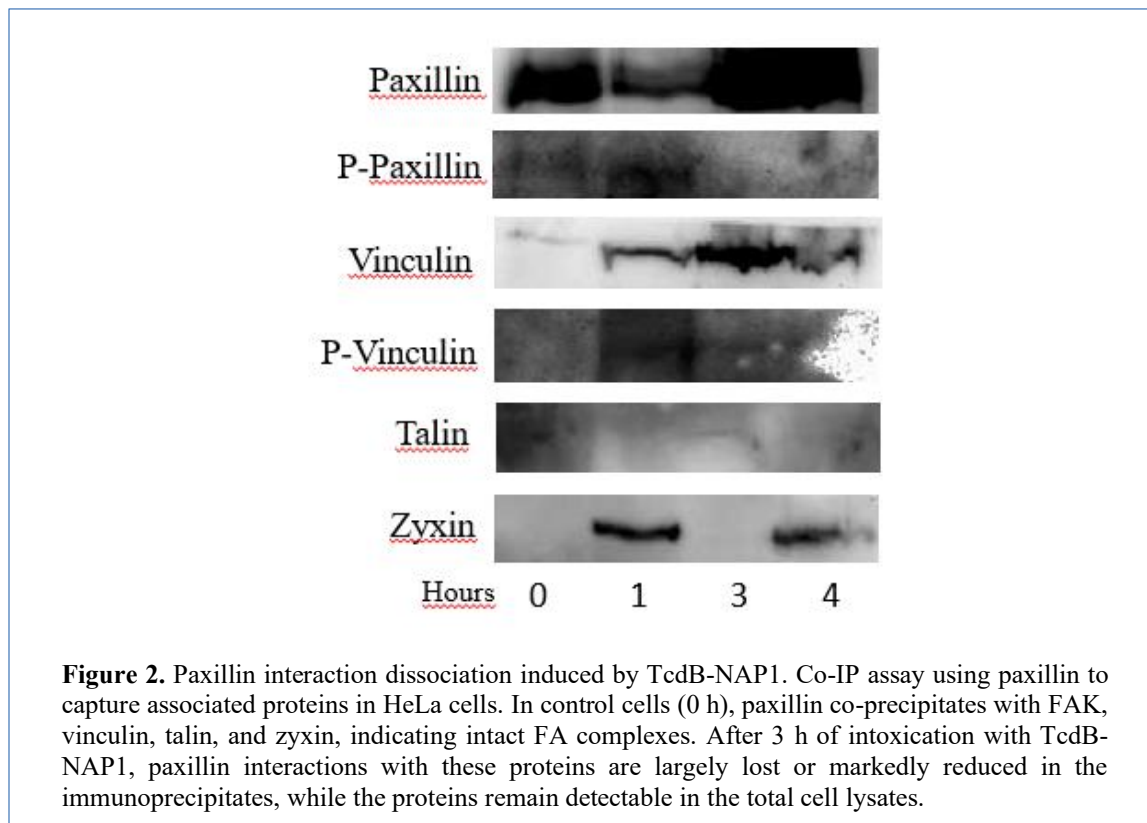


**Figure 1.** Structural protein integrity in cell adhesions after TcdB variant intoxication. WB analysis of total HeLa cell lysates intoxicated with TcdB-VPI, TcdB-NAP1, and TcdB-NAP1v over 0, 30 min, 1, 2, 3, and 4 h. (A) Plectin detection shows a progressive decrease in signal under RhoA-inactivating conditions. (B) ZO-1 detection remains stable across all time points and conditions. (C) Talin detection is constant throughout intoxication, suggesting that structural focal adhesion components are not subject to massive degradation.  $\alpha$ -actin was used as a loading control (data not shown).

Furthermore, a significant decrease in the intensity of the phosphorylated paxillin (p-paxillin) band was observed between 2 and 3 hours of intoxication with the RhoA-inactivating variants (VPI and NAP1), while this marker remained stable in HeLa cells exposed to TcdB-NAP1v. Conversely, other phosphorylated forms, such as P-Src and P-zyxin, exhibited no discernible alterations in their banding patterns under any of the intoxication conditions.

### *Paxillin protein interactions by Co-IP*

After 3 hours of intoxication with TcdB-NAP1, changes in the Co-IP pattern were observed, as the bands corresponding to FAK, vinculin, talin, and zyxin showed reduced intensity or were absent from the paxillin pull-down compared to untreated samples (Fig. 2). Thus, paxillin, vinculin, and zyxin were detected in the total lysates, thereby confirming their presence under all conditions. Conversely, the Co-IP fraction exhibited a significant decrease or absence of Vinculin and Zyxin associated with Paxillin following intoxication, suggesting a biochemical disassembly of focal adhesion complexes.



Additionally, phosphorylated paxillin (P-paxillin) was no longer detectable in the precipitated complex after exposure to TcdB-NAP1. These results demonstrate that TcdB-NAP1 intoxication induces the dissociation of proteins physically associated with paxillin (Fig. 3).

Densitometric quantification of the WB bands confirmed these observations, revealing a significant time-dependent reduction of proteins and phosphorylated proteins following exposure to toxins TcdB-VPI and TcdB-NAP1, whereas no significant changes were detected in cells treated with TcdB-NAP1v (Tables S1–S2,  $p < 0.05$ ).

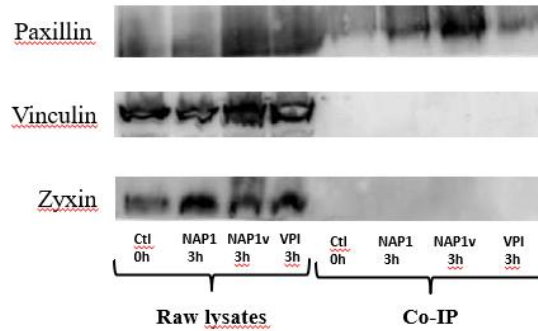


**Figure 3.** Disruption of the paxillin interactome induced by TcdB toxins. Co-IP assay using a monoclonal anti-Paxillin antibody coupled to Protein G beads in HeLa cells, either untreated (0 h) or intoxicated for 3 hours with TcdB from NAP1, NAP1v, and VPI strains.

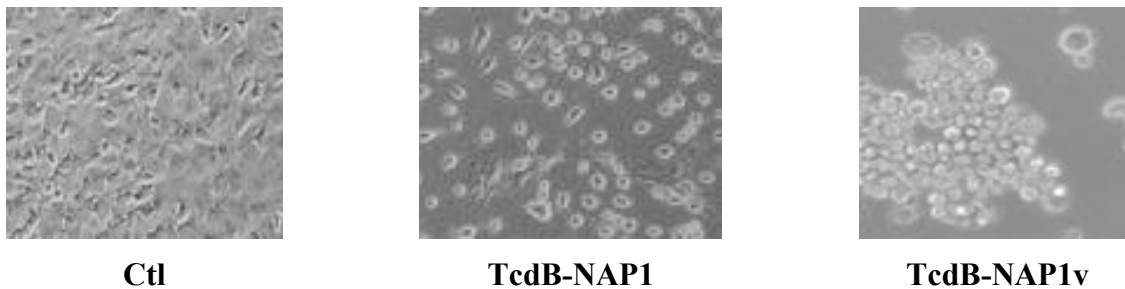


**Figure 4.** Differential cytopathic effects (CPE) induced by TcdB variants in HeLa cells. Representative micrographs obtained by light microscopy after 4 hours of exposure to a standardized 50 ng/well dose. (Ctl) Untreated control cells displaying normal fusiform morphology and confluence. (TcdB-NAP1) Cell rounding phenotype (classical CPE). (TcdB-NAP1v) Arborizing phenotype characterized by cytoplasmic projections (variant CPE).

## DISCUSSION

A comprehensive understanding of *C. difficile* pathogenesis requires elucidating the physical disassembly of cellular structures. A comparison of TcdB variants has been shown to reveal a direct correlation between molecular substrate specificity and the observed cytopathic phenotype. TcdB-VPI and TcdB-NAP1 have been shown to inactivate RhoA, Rac1, and Cdc42, while the TcdB-NAP1v variant has been observed to lack the glycosylating capability of the other two<sup>19</sup>.

This functional divergence elucidates the basis for NAP1v's propensity to induce a rounding phenotype, bearing resemblance to the effect of *C. sordellii* lethal toxin, in contrast to the arborizing effect characteristic of the classical strains. These findings are consistent with previous reports, as exposure to TcdB leads to disruption of cellular organization, similar to that described for TcdA and TcdB provoke disassembly and condensation of the cytoskeleton in human colonic epithelium<sup>20,21</sup>. In polarized epithelial cells, cytoskeletal depolymerization also leads to disorganization of adherens junctions.

In this study, HeLa cells were utilized as the primary experimental model, a choice justified by several technical and biological considerations. Although TcdB primarily targets the intestinal

epithelium, HeLa cells are a well-established standard in *C. difficile* toxicology due to their robust and stable expression of key TcdB receptors, specifically CSPG4 and FZD<sup>1, 2, and 7</sup>. CSPG4 has been identified as a dominant receptor for clade 2 TcdB variants, such as those analyzed here, making HeLa cells a highly sensitive and relevant system for dissecting early molecular events in the adhesome.

The toxin concentration of 50 ng/well was selected based on previously published dose–response and time-course characterizations of TcdB in HeLa cells reported previously<sup>12</sup>, who performed systematic toxin titrations and described comparable cytopathic kinetics in this cell line, with visible CPE developing within hours at effective concentrations. After adapting those published titration conditions to the toxin stocks and well format used in the present study, 50 ng/well was established as an empirically effective concentration for the comparative experiments described here.

For instance, lethal toxins from *C. sordellii* have been shown to induce internalization of E-cadherin/ $\beta$ -catenin complexes and disorganization of basolateral actin<sup>22</sup>. Therefore, the disruption of actin filaments associated with adhesions signifies the disassembly of focal and adherent adhesion complexes, thereby weakening cellular attachments. Structures such as focal adhesions, which include adaptor proteins like talin, vinculin,  $\alpha$ -actinin, and paxillin, are particularly compromised<sup>23, 24</sup>.

In this context, paxillin functions as a marker of focal adhesion status, and tyrosine phosphorylation of paxillin typically indicates adhesions that are forming or undergoing dynamic remodeling. While paxillin constitutes merely a single component of the adhesome, its role in cellular adhesions is pivotal. Its phosphorylation can indirectly reflect the activity of Rho GTPases<sup>23,25,26</sup>. In the present study, paxillin was selected for analysis due to its established correlation with focal adhesion assembly, though it should be noted that other pivotal proteins, such as FAK, vinculin, and talin, may also be subject to alteration. The limitation of assessing only paxillin in the Co-IP experiments was primarily technical and based on its role as the most sensitive indicator of focal adhesion structure, rather than implying it is the only relevant target. A central finding is that the collapse of focal adhesions does not result from massive proteolytic degradation of their components, but rather from a systemic failure in their assembly and organization. The stability observed by Western Blot for proteins such as talin, zyxin, and ZO-1 indicates that the structural components remain within the cell.

However, the loss of physical interaction revealed by Co-IP for paxillin shows that these elements undergo redistribution from the cell periphery. In the case of ZO-1, its displacement from the lateral membrane toward the cytosol occurs in parallel with actin disorganization. The retention of talin, which directly links integrin tails to the cytoskeleton, and zyxin as intact bands in the WB, despite their disappearance from the paxillin pull-down, reinforces the notion that the toxin induces a decoupling of the physical anchors between integrins and the cytoskeleton<sup>27</sup>.

Moreover, the differential behavior observed in the two conditions yielded distinct phenotypes. The variant toxin induced an arborizing cytopathic effect, characterized by thin actin extensions, whereas the other caused classical cell rounding without prominent protrusions. This morphological contrast aligns with previous studies showing that certain TcdB variants that do not glucosylate RhoA produce an arborized phenotype, while those that inactivate RhoA lead to complete rounding<sup>28</sup>. Our assays showed that the strain with intact RhoA generated actin protrusions, whereas the other caused fiber collapse, indicating that RhoA inactivation underlies the rounded morphology. This morphological difference underscores that the toxin's substrate specificity, specifically which GTPase it inactivates, determines the resulting cellular phenotype<sup>29</sup>.

The disruption of these adhesion complexes has functional consequences for the cell. Specifically, the loss of FAK–Paxillin signaling and the disorganization of the actin and intermediate filament network accentuate cell rounding. Furthermore, these changes may facilitate processes such as epithelial barrier destabilization or cell motility. The results of this study suggest a decrease in adhesion-associated signals, indicating that adaptor proteins within these complexes are affected<sup>19,30</sup>.

The changes observed in paxillin are consistent with a biochemical disassembly of cell–matrix adhesion complexes rather than a direct structural rupture<sup>31,32</sup>. Therefore, in addition to protein disruption, a biochemical disassembly affecting integrin–actin junctions were evident, leaving the cell unable to maintain its normal adherent structure. The selection of NAP1 as the sole variant for the Co-IP assays is justified by the mechanistic redundancy observed among RhoA-inactivating toxins. Since VPI and NAP1 induce the same negative signaling cascade on the paxillin interactome, the Co-IP results obtained with NAP1 provide a valid molecular framework for both. In contrast, the NAP1v variant, by not glucosylating RhoA, preserves the basal signaling of focal adhesions, making its analysis by Co-IP unnecessary for validating the proposed disassembly model, which appears to be a signature exclusive to variants that collapse RhoA activity.

In contrast to the other proteins, plectin exhibited a distinctive quantitative decrease, as evidenced by the quantitative analysis. This protein is indispensable for anchoring intermediate filaments to focal adhesions, thereby playing a pivotal role in cell motility and invasion. Its loss suggests that the toxins undermine cellular integrity in a multidimensional manner, potentially affecting both microfilaments and intermediate filaments<sup>33</sup>. It can be hypothesized that the degradation of plectin is mediated by calpains activated by calcium flux. Calpain-2 is known to regulate FAK proteolysis in a Src phosphorylation–dependent manner<sup>34</sup>.

The capacity of NAP1 to disrupt adhesion complexes, in conjunction with its enhanced autoproteolysis, suggests a potential correlation with the clinical severity of the condition. The disintegration of focal adhesions undermines their function in transmitting force or tension to adhesion sites, resulting in diarrhea and subjecting the epithelium to inflammation<sup>35</sup>.

## CONCLUSION

This study appears to support the model in which clostridial toxins induce actin depolymerization and the collapse of cellular adhesions through the inactivation of Rho GTPases<sup>36</sup>. Although altered paxillin phosphorylation may not be the primary cause of this disruption, it serves as a marker of the disruption and reflects the state of the adhesome after signaling is interrupted<sup>37</sup>. In the context of *C. difficile* infection, these findings suggest that the toxins selectively disrupt focal adhesions, compromising epithelial integrity beyond the visible morphological changes.

Finally, the functional disruption of key cell-matrix adhesion complexes suggests a potential mechanism for cell detachment and mucosal damage, which are hallmarks of *C. difficile*-associated colitis. Additionally, the observed differences between conventional and variant toxins highlight how substrate specificity influences the extent of epithelial injury and may affect the severity of the disease.

## Acknowledgements

We would like to acknowledge the technical assistance provided by Pablo Vargas. We would also like to express our gratitude to the LIBA-UCR staff for their invaluable assistance with the experiments.

## Authors' contributions

DLR, IJB: experimental design, performed experiments, analyzed data. CQG: experimental design, provided reagents, performed experiments, supervision.

## Funding

This study was funded by the Vice-Rectoría for Research at the University of Costa Rica (grants B9450 and B7183).

## Conflict of interest

The authors declare that they have no conflict of interest.

## REFERENCES

1. Bilverstone TW, Garland M, Cave RJ, Kelly ML, Tholen M, Bouley DM, Kaye P, Minton NP, Bogyo M, Kuehne SA, Melnyk RA. The glucosyltransferase activity of *C. difficile* Toxin B is required for disease pathogenesis. *PLoS Pathogens*. 2020;16(9):e1008852. doi:10.1371/journal.ppat.1008852
2. Liu C, Monaghan T, Yadegar A, Louie T, Kao D. Insights into the evolving epidemiology of *Clostridioides difficile* infection and treatment: a global perspective. *Antibiotics*. 2023;12(7):1141. doi:10.3390/antibiotics12071141
3. Quesada-Gómez C, López-Ureña D, Chumbler N, Kroh HK, Castro-Peña C, Rodríguez C, Orozco-Aguilar J, González-Camacho S, Rucavado A, Guzmán-Verri C, Lawley TD. Analysis of TcdB proteins within the hypervirulent clade 2 reveals an impact of RhoA glucosylation on *Clostridium difficile* proinflammatory activities. *Infection and Immunity*. 2016;84(3):856-65. doi:10.1128/iai.01291-15
4. Li Z, Shao R, Xin H, Zhu Y, Jiang S, Wu J, Yan H, Jia T, Ge M, Shi X. Paxillin and kindlin: research progress and biological functions. *Biomolecules*. 2025;15(2):173. doi:10.3390/biom15020173
5. Klapholz B, Brown NH. Talin—the master of integrin adhesions. *Journal of Cell Science*. 2017;130(15):2435-46. doi:10.1242/jcs.190991
6. Legerstee K, Houtsmuller AB. A layered view on focal adhesions. *Biology*. 2021;10(11):1189. doi:10.3390/biology10111189
7. Huang J, Kelly CP, Bakirtzi K, Villafuerte Gálvez JA, Lyras D, Mileto SJ, Larcombe S, Xu H, Yang X, Shields KS, Zhu W. *Clostridium difficile* toxins induce VEGF-A and vascular permeability to promote disease pathogenesis. *Nature Microbiology*. 2019;4(2):269-79. doi:10.1038/s41564-018-0300-x
8. Pourliotopoulou E, Karampatakis T, Kachrimanidou M. Exploring the toxin-mediated mechanisms in *Clostridioides difficile* infection. *Microorganisms*. 2024;12(5):1004. doi:10.3390/microorganisms12051004
9. Quesada-Gómez C, López-Ureña D, Acuña-Amador L, Villalobos-Zúñiga M, Du T, Freire R, Guzmán-Verri C, Gamboa-Coronado MD, Lawley TD, Moreno E, Mulvey MR. Emergence of an outbreak-associated *Clostridium difficile* variant with increased virulence. *Journal of Clinical Microbiology*. 2015;53(4):1216-26. doi:10.1128/jcm.03058-14
10. Hamo Z, Azrad M, Fichtman B, Peretz A. The cytopathic effect of different toxin concentrations from different *Clostridioides difficile* sequence types strains in Vero cells. *Frontiers in Microbiology*. 2021;12:763129. doi: 10.3389/fmicb.2021.763129

11. Tam J, Beilhartz GL, Auger A, Gupta P, Therien AG, Melnyk RA. Small molecule inhibitors of Clostridium difficile toxin B-induced cellular damage. *Chemistry & Biology*. 2015;22(2):175-85. doi:10.1016/j.chembiol.2014.12.010
12. López-Ureña D, Orozco-Aguilar J, Chaves-Madrigal Y, Ramírez-Mata A, Villalobos-Jimenez A, Ost S, Quesada-Gómez C, Rodríguez C, Papatheodorou P, Chaves-Olarte E. Toxin B variants from Clostridium difficile strains VPI 10463 and NAP1/027 share similar substrate profile and cellular intoxication kinetics but use different host cell entry factors. *Toxins*. 2019;11(6):348. doi:10.3390/toxins11060348
13. Stieglitz F, Gerhard R, Hönig R, Giehl K, Pich A. TcdB of Clostridioides difficile mediates RAS-dependent necrosis in epithelial cells. *International Journal of Molecular Sciences*. 2022;23(8):4258. doi:10.3390/ijms23084258
14. Chumbler NM, Farrow MA, Lapierre LA, Franklin JL, Haslam D, Goldenring JR, Lacy DB. Clostridium difficile toxin B causes epithelial cell necrosis through an autoproducting-independent mechanism. *PLoS pathogens*. 2012;8(12):e1003072. doi:10.1371/journal.ppat.1003072
15. Genth H, Huelsenbeck J, Hartmann B, Hofmann F, Just I, Gerhard R. Cellular stability of Rho-GTPases glucosylated by Clostridium difficile toxin B. *FEBS letters*. 2006;580(14):3565-9. doi:10.1016/j.febslet.2006.04.100
16. Stieglitz F, Gerhard R, Hönig R, Giehl K, Pich A. TcdB of Clostridioides difficile mediates RAS-dependent necrosis in epithelial cells. *International Journal of Molecular Sciences*. 2022;23(8):4258. doi:10.3390/ijms23084258
17. Edwards M, McConnell P, Schafer DA, Cooper JA. CPI motif interaction is necessary for capping protein function in cells. *Nature Communications*. 2015;6(1):8415. doi:10.1038/ncomms9415
18. Xue Q, Varady SR, Waddell TQ, Roman MR, Carrington J, Roh-Johnson M. Lack of Paxillin phosphorylation promotes single-cell migration in vivo. *Journal of Cell Biology*. 2023;222(3):e202206078. doi:10.1083/jcb.202206078
19. Sun X, Savidge T, Feng H. The enterotoxicity of Clostridium difficile toxins. *Toxins*. 2010;2(7):1848-80. doi:10.3390/toxins2071848
20. Riegler M, Sedivy R, Pothoulakis C, Hamilton G, Zacherl J, Bischof G, Cosentini E, Feil W, Schiessel R, LaMont JT. Clostridium difficile toxin B is more potent than toxin A in damaging human colonic epithelium in vitro. *Journal of Clinical Investigation*. 1995;95(5):2004-11. doi:10.1172/JCI117885
21. Di Bella S, Ascenzi P, Siarakas S, Petrosillo N, Di Masi A. Clostridium difficile toxins A and B: insights into pathogenic properties and extraintestinal effects. *Toxins*. 2016;8(5):134. doi:10.3390/toxins8050134
22. Boehm C, Gibert M, Geny B, Popoff MR, Rodriguez P. Modification of epithelial cell barrier permeability and intercellular junctions by Clostridium sordellii lethal toxins. *Cellular Microbiology*. 2006;8(7):1070-85.
23. Zaidel-Bar R, Itzkovitz S, Ma'ayan A, Iyengar R, Geiger B. Functional atlas of the integrin adhesome. *Nature Cell Biology*. 2007;9(8):858-67. doi:10.1038/ncb0807-858
24. Boehm C, Gibert M, Geny B, Popoff MR, Rodriguez P. Modification of epithelial cell barrier permeability and intercellular junctions by Clostridium sordellii lethal toxins. *Cellular Microbiology*. 2006;8(7):1070-85. doi:10.1111/j.1462-5822.2006.00687.x
25. Pasapera AM, Schneider IC, Rericha E, Schlaepfer DD, Waterman CM. Myosin II activity regulates vinculin recruitment to focal adhesions through FAK-mediated paxillin phosphorylation. *Journal of Cell Biology*. 2010;188(6):877-90. doi:10.1083/jcb.200906012
26. Geny B, Grassart A, Manich M, Chicanne G, Payrastre B, Sauvonnnet N, Popoff MR. Rac1 inactivation by lethal toxin from Clostridium sordellii modifies focal adhesions upstream of actin

- depolymerization. *Cellular Microbiology*. 2010;12(2):217-32. doi:10.1111/j.1462-5822.2009.01392.x
27. Nusrat A, von Eichel-Streiber C, Turner JR, Verkade P, Madara JL, Parkos CA. Clostridium difficile toxins disrupt epithelial barrier function by altering membrane microdomain localization of tight junction proteins. *Infection and Immunity*. 2001;69(3):1329-36. doi:10.1128/iai.69.3.1329-1336.2001
  28. Chaves-Olarte E, Freer E, Parra A, Guzmán-Verri C, Moreno E, Thelestam M. R-Ras glucosylation and transient RhoA activation determine the cytopathic effect produced by toxin B variants from toxin A-negative strains of Clostridium difficile. *Journal of Biological Chemistry*. 2003;278(10):7956-63. doi:10.1074/jbc.M209244200
  29. May M, Wang T, Müller M, Genth H. Difference in F-actin depolymerization induced by toxin B from the Clostridium difficile strain VPI 10463 and toxin B from the variant Clostridium difficile serotype F strain 1470. *Toxins*. 2013;5(1):106-19. doi:10.3390/toxins5010106
  30. Kim H, Rhee SH, Pothoulakis C, LaMont JT. Clostridium difficile toxin A binds colonocyte Src causing dephosphorylation of focal adhesion kinase and paxillin. *Experimental Cell Research*. 2009;315(19):3336-44. doi:10.1016/j.yexcr.2009.05.020
  31. Cortesio CL, Boateng LR, Piazza TM, Bennin DA, Huttenlocher A. Calpain-mediated proteolysis of paxillin negatively regulates focal adhesion dynamics and cell migration. *Journal of Biological Chemistry*. 2011;286(12):9998-10006. doi:10.1074/jbc.M110.187294
  32. Hage B, Meinel K, Baum I, Giehl K, Menke A. Rac1 activation inhibits E-cadherin-mediated adherens junctions via binding to IQGAP1 in pancreatic carcinoma cells. *Cell Communication and Signaling*. 2009;7(1):23. doi:10.1186/1478-811X-7-23
  33. Wiche G. Plectin-mediated intermediate filament functions: why isoforms matter. *Cells*. 2021;10(8):2154. doi.org/10.3390/cells10082154
  34. Chan KT, Bennin DA, Huttenlocher A. Regulation of adhesion dynamics by calpain-mediated proteolysis of focal adhesion kinase (FAK). *Journal of Biological Chemistry*. 2010;285(15):11418-26. doi:10.1074/jbc.M109.090746
  35. Lanis JM, Hightower LD, Shen A, Ballard JD. TcdB from hypervirulent Clostridium difficile exhibits increased efficiency of autoprocessing. *Molecular Microbiology*. 2012;84(1):66-76. doi:10.1111/j.1365-2958.2012.08009.x
  36. Aktories K, Schwan C, Jank T. Clostridium difficile toxin biology. *Annual Review of Microbiology*. 2017;71:281-307. doi:10.1146/annurev-micro-090816-093458
  37. Cheng SY, Sun G, Schlaepfer DD, Pallen CJ. Grb2 promotes integrin-induced focal adhesion kinase (FAK) autophosphorylation and directs the phosphorylation of protein tyrosine phosphatase  $\alpha$  by the Src-FAK kinase complex. *Molecular and Cellular Biology*. 2014;34(3):348-61. doi:10.1128/MCB.00825-13